

# A way around the exponential scaling in optimal quantum control

Modesto Orozco-Ruiz,<sup>1</sup> Nguyen H. Le,<sup>1</sup> and Florian Mintert<sup>1</sup>

<sup>1</sup>*Physics Department, Blackett Laboratory, Imperial College London,  
Prince Consort Road, SW7 2AZ, United Kingdom*

We show that combining ideas from the fields of quantum invariants and of optimal control can be used to design quantum control of quantum systems without explicit reference to quantum states. The scaling in numerical effort of the resultant approach is given by commutation relations of system operators, and it can be polynomial in the number of subsystems despite the general quantum mechanical exponential scaling of the Hilbert space. As explicit applications, we discuss state preparation and quantum simulation with Hamiltonians including three-body and many-body interactions with spin chains of up to 50 constituents, and the perspective of use for topologically protected quantum information processing.

## I. INTRODUCTION

The availability of well-controlled quantum systems offers the prospect towards a broad range of applications, including quantum simulation [1, 2] and quantum computation [3, 4]. The exponential growth of the Hilbert space in such systems suggests that even moderately small quantum systems could be employed to achieve tasks that would be impractical to perform classically [5, 6]. While the benefits of this scaling have inspired tremendous efforts towards the development of quantum technological devices [5, 7–9], the scaling also has disastrous implications on our abilities to simulate the dynamics of quantum systems [10].

Most attempts to devise control schemes of quantum systems are thus restricted to exact analyses performed on small systems [11, 12] with potential extensions to larger system via approximate techniques [13, 14], specific systems that admit efficient descriptions [15, 16], or, to analyses that are approximate to start with [17]. While this exponential scaling seems an insurmountable obstacle in general, there are specific instances of quantum states that can be described with an effort that scales more favourably than exponentially [18, 19].

A very efficient, even though implicit way of describing some quantum states is given in terms of the operator (or operators) to which a state is an eigenstate [20]. There is, for example, a large variety of quantum many-body Hamiltonians with highly complicated ground states [21–23]. The Hamiltonian is typically specified very efficiently in terms of the interaction geometry and the type of interaction mechanism. Even though the explicit specification of the ground state of such a Hamiltonian is hardly ever efficient, the implicit specification via the Hamiltonian is.

While ideas to characterize quantum states in terms of operators to which they are eigenstates do exist [24], optimal control seems to exclusively focus on explicit descriptions of state vectors [25]. The goal of this paper is to demonstrate that optimal control can be realized without explicit construction of quantum states, and that this can make control problems numerically accessible whose realization based on explicit state vector descriptions are prohibitively expensive.

The underlying idea is inspired by the framework of quantum invariants [26–28], *i.e.* hermitian operators  $\mathcal{I}(t)$  with a vanishing total time-derivative, *i.e.*

$$\frac{d\mathcal{I}}{dt} = \frac{\partial\mathcal{I}}{\partial t} + i[H(t), \mathcal{I}(t)] = 0 . \quad (1)$$

Each such invariant has instantaneous eigenvectors, *i.e.* generally time-dependent vectors satisfying the eigenvalue relation

$$\mathcal{I}(t) |\Psi(t)\rangle = \lambda |\Psi(t)\rangle . \quad (2)$$

Due to the unitary dynamics resultant from Eq. (1), any eigenvalue  $\lambda$  of  $\mathcal{I}(t)$  is time-independent.

Since every non-degenerate, instantaneous eigenvector specifies a solution of the time-dependent Schrödinger equation with the time-dependent Hamiltonian  $H(t)$  [26], invariants are commonly used tools in optimal quantum control [29].

Existing use of quantum invariants in optimal quantum control is based on the identification of analytic time-dependences that make an operator satisfy Eq. (1) for a certain type of Hamiltonian, such as the driven harmonic oscillator Hamiltonian and the Hamiltonian of a single driven spin [30–32]. Once such an analytic form is identified, the resultant invariant provides very elegant means of engineering a time-dependent Hamiltonian that induces desired dynamics. It does, however, seem elusive to generalize this analytic approach to more complicated systems such as interacting spins.

Our present goal is thus to develop a framework in the spirit of numerical quantum control [4, 33] that does not rely on the existence of analytic solutions, but that avoids reference to quantum states whose description would require an exponential effort.

## II. IMPLICIT QUANTUM CONTROL

Instead of numerically propagating the Schrödinger equation explicitly for a time-dependent state vector, the proposed approach relies on numerically propagating Eq. (1) for an operator  $\mathcal{I}(t)$ . Following the eigenvalue relation Eq.(2), this provides all information on the desired

state vector, but as long as  $\mathcal{I}(t)$  is not diagonalised, this information remains implicit.

The goal of this manuscript is to show how to define a control target  $\mathcal{I}_T$  for an operator  $\mathcal{I}(t)$  following the dynamics of Eq. (1), such that numerical pulse shaping techniques can be applied to Eq. (1), and such that the resultant Hamiltonian induces desired dynamics in the underlying Schrödinger equation.

While translating a control problem from the Schrödinger equation to the corresponding Liouville-von Neumann equation, *i.e.* Eq. (1), does in general not provide any improvement in efficiency, there are indeed instances such as Eqs. (20) and (21) discussed in more detail below, and a series of further examples listed in Sec. V for which this translation results in an exponential improvement.

### A. Operator expansion

The crucial aspect to determine whether the present approach is more efficient than approaches based on state vectors is the effort required to perform the propagation of  $\mathcal{I}(t)$  following Eq. (1).

Since there is a multitude of different operators with the same ground-state, there is no unique choice for the initial condition  $\mathcal{I}(0)$  to represent a given initial state  $|\Psi(0)\rangle$ , and this freedom can be used to find an initial condition  $\mathcal{I}(0)$  that allows for a particularly efficient propagation.

Formalization of this statement requires the definition of system Hamiltonian. In the following, it is considered to be of the form

$$H(t) = \sum_j h_j \mathfrak{h}_j, \quad (3)$$

spanned by a set of operators  $\mathfrak{h}_j$  with scalar expansion coefficients  $h_j$ . Some of those can be time-independent and fixed (as in a drift Hamiltonian), but some should be time-dependent and tuneable (as in a control Hamiltonian).

The operator

$$\mathcal{I} = \sum_{j=1}^d a_j \mathfrak{a}_j, \quad (4)$$

to be propagated, is expanded into a set of time-independent operators  $\mathfrak{a}_j$  with time-dependent scalar expansion coefficients  $a_j$ . This Ansatz can help to solve the equation of motion Eq.(1), only if the set of operators  $\{\mathfrak{a}_j\}$  is closed under commutation with any of the operators  $\mathfrak{h}_k$ , *i.e.* if any commutator  $[\mathfrak{a}_j, \mathfrak{h}_k]$  can be expanded in terms of the set  $\{\mathfrak{a}_j\}$ , such that

$$[\mathfrak{a}_j, \mathfrak{h}_k] = -i \sum_{l=1}^d \lambda_{jl}^k \mathfrak{a}_l. \quad (5)$$

In any finite-dimensional system, this condition can always be satisfied, if the set of operators is chosen to have sufficiently many elements, but in the following, it will be crucial that the set  $\{\mathfrak{a}_j\}$  is sufficiently small.

If the sets of operators  $\{\mathfrak{a}_j\}$  and  $\{\mathfrak{h}_k\}$  coincide, the present discussion reduces to the common structure of a Lie algebra, but in order to find small sets of operators  $\{\mathfrak{a}_j\}$  it can be beneficial to consider situations beyond Lie algebras.

### B. Equations of motion

With the explicit expansion in terms of the sets of operators  $\{\mathfrak{a}_j\}$  and  $\{\mathfrak{h}_k\}$ , the equation of motion Eq. (1) reads [34]

$$\frac{\partial \mathcal{I}}{\partial t} = i \sum_{j,k} a_j h_k [\mathfrak{a}_j, \mathfrak{h}_k] = \sum_{j,k,l} a_j h_k \lambda_{jl}^k \mathfrak{a}_l. \quad (6)$$

Since the set of operators  $\mathfrak{a}_j$  is linearly independent, this implies the differential equation

$$\dot{\mathbf{a}} = \sum_{j,k} a_j h_k \lambda_{jl}^k, \quad (7)$$

that can be written compactly as

$$\dot{\mathbf{a}} = K(t) \mathbf{a}, \quad (8)$$

with the vector  $\mathbf{a}$  and a matrix  $K$  with elements

$$K_{jl} = \sum_k h_k \lambda_{jl}^k. \quad (9)$$

The hermitian operators  $\mathfrak{a}_j$  can always be chosen to be mutually orthonormal, such that Eq. (5) implies

$$\lambda_{jl}^k = i \operatorname{tr}([\mathfrak{a}_j, \mathfrak{h}_k] \mathfrak{a}_l). \quad (10)$$

Invariance of the trace under cyclic permutation implies

$$\lambda_{jl}^k = i \operatorname{tr}([\mathfrak{a}_l, \mathfrak{a}_j] \mathfrak{h}_k) = -\lambda_{lj}^k. \quad (11)$$

In this case, the matrix  $K$  is real and anti-symmetric [31] such that the induced dynamics is orthogonal, *i.e.* unitary and real.

### C. Formulation of the control problem

If formulated in terms of Eq. (8) instead of the underlying Schrödinger equation, the dimension of the dynamics underlying the control problem is given by the size  $d$  of the set of operators  $\{\mathfrak{a}_j\}$ , and not by the dimension of the underlying Hilbert space.

In general,  $d$  can be quadratically larger than the size of the Hilbert space, but as exemplified in the following, there are several instances of practical importance

in which  $d$  is much smaller. The goal of the following discussion is to benefit from this reduced dimensionality for optimal control problems.

While typically control problems are defined in terms of a target state or a target gate, the present framework requires a control target for the operator  $\mathcal{I}$ , and defining this requires some care. In the following, we will discuss this for the problems of diabatic transitions between eigenstates of two operators and for the realization of a desired unitary.

### 1. Diabatic transitions

The problem of diabatic transitions is a natural application of the present framework, because Hamiltonians can typically be specified efficiently, whereas the explicit specification of their eigenstates is often not efficient.

For the problem of finding a time-dependent Hamiltonian such that the system evolves from the ground-state of an initial operator  $H_I$  to the ground-state of a final operator  $H_F$ , it seems tempting to define the initial condition  $\mathcal{I}(0) = H_I$  and the control target  $\mathcal{I}_T = H_F$ . However, since the spectrum of  $\mathcal{I}(t)$  is time-independent, this would necessarily imply the restriction that  $H_I$  and  $H_F$  have the same spectrum.

In addition to the natural requirements that

- (i) the initial condition  $\mathcal{I}(0)$  needs to be specified such that the initial state  $|\Psi_1\rangle$  (an eigenvector of  $H_I$ ) is an eigenstate of  $\mathcal{I}(0)$  with a non-degenerate eigenvalue  $\gamma$ ; and that
- (ii) the control target  $\mathcal{I}_T$  needs to be chosen such that the target state  $|\Psi_2\rangle$  (an eigenvector of  $H_F$ ) is an eigenstate of  $\mathcal{I}_T$  with the same eigenvalue  $\gamma$ ,

there is thus the third requirement that

- (iii) the control target needs to be reachable with the dynamics induced by the control Hamiltonian  $H(t)$ , *i.e.*, the dynamics following Eq. (8).

If the choice  $\mathcal{I}(0) = H_I$  is taken, one can consider an adiabatic transition from  $H_I$  to  $H_F$ , and simulating the adiabatic evolution in Eq. (8) yields a final invariant that is reachable with the available dynamics and that has  $|\Psi_2\rangle$  as eigenstate. While such a numerical construction is a generally applicable approach, there are also instances in which suitable control targets can be defined analytically as exemplified in Secs. III B 1 and III B 2.

Given a consistent definition for initial condition  $\mathcal{I}(0)$  and control target  $\mathcal{I}_T$ , a generic choice for objective function is the infidelity

$$\mathcal{J} = 1 - \frac{\text{tr}(\mathcal{I}(T)\mathcal{I}_T)}{\text{tr}(\mathcal{I}_T^2)}, \quad (12)$$

where  $T$  is the final time at which the goal of the control problem is intended to be reached. Since the infidelity is

readily expressed as

$$\mathcal{J} = 1 - \frac{\mathbf{a}(T) \cdot \mathbf{a}_T}{\|\mathbf{a}_T\|^2}, \quad (13)$$

with the vector  $\mathbf{a}_T$  of the control target  $\mathcal{I}_T$ , the effort to evaluate the infidelity scales with the dimension  $d$  and not with the dimension of system's Hilbert space.

### 2. Desired unitary

In contrast to the above problem of diabatic transitions, there is no ambiguity in defining the target operator  $\mathcal{I}_T$  corresponding to an initial condition  $\mathcal{I}(0)$  for the control problem of realizing a desired unitary  $\mathcal{U}_T$ . The problem is that optimizing for an objective function  $\mathcal{I}_T = \mathcal{U}_T\mathcal{I}(0)\mathcal{U}_T^\dagger$  does not ensure that the desired unitary is actually achieved.

An objective function such that its optimal value unambiguously verifies the realization of the desired unitary  $\mathcal{U}_T$  requires a set of  $N_c$  initial conditions  $\mathcal{I}_j(0)$  and corresponding targets  $\mathcal{I}_{T,j} = \mathcal{U}_T\mathcal{I}_j(0)\mathcal{U}_T^\dagger$ . However, only with a sufficiently large number of these initial conditions does the objective function,

$$\mathcal{J}_{\mathcal{U}_T} = 1 - \frac{1}{N_c} \sum_{j=1}^{N_c} \frac{\text{tr}(\mathcal{I}_j(T)\mathcal{U}_T\mathcal{I}_j(0)\mathcal{U}_T^\dagger)}{\text{tr}((\mathcal{I}_j(0))^2)} \quad (14)$$

guarantee that a vanishing value of  $\mathcal{J}_{\mathcal{U}_T}$  unambiguously implies the realized unitary coincides with the desired unitary  $\mathcal{U}_T$ .

While, in general, the gate-infidelity  $\mathcal{J}_{\mathcal{U}_T}$  would require an exponentially large set of initial conditions, the fact that the dynamics takes place in a Lie group of small size also permits to define a faithful target that requires a correspondingly small number of initial conditions, as exemplified further down in Sec. IV A. With each summand in Eq. (14) evaluated analogously to Eq. (12), the objective function  $\mathcal{J}_{\mathcal{U}_T}$  can thus be evaluated with polynomial effort.

### 3. Numerical optimization

Once a control target  $\mathcal{I}_T$  and an objective function, such as  $\mathcal{J}$  (Eq. (12)) or  $\mathcal{J}_{\mathcal{U}_T}$  (Eq. (14)) is specified, one can use any numerical pulse shaping algorithm [35] to design a time-dependent Hamiltonian that realizes a dynamics from  $\mathcal{I}(0)$  to  $\mathcal{I}(T)$ , at a final time  $T$ , that is close to  $\mathcal{I}_T$ . Since Eq. (8) with an anti-symmetric matrix  $K$  induces orthogonal (unitary and real) dynamics, any numerical algorithm that is applicable to the Schrödinger equation (such as Krotov [36], GRAPE [11] or CRAB [14]) is directly applicable, and techniques to construct *e.g.* gradients with respect to control parameters also directly apply to Eq. (8).

Since any such optimization is based on numerically exact integration of Eq. (8), there is no restriction to adiabaticity, and the duration  $T$  of the control protocol can be chosen as short as allowed by the physical constraints of the underlying system.

Mere continuity implies that in the limit of vanishing infidelity  $\mathcal{J}$  for the non-degenerate operator  $\mathcal{I}(T)$  also the infidelity of the realized quantum state approaches its ideal value. Beyond this qualitative assessment, also a more quantitative estimate can be obtained in terms of the spectrum of  $H_F$ .

To this end, the final state  $|\psi(T)\rangle$  can be expressed as

$$|\psi(T)\rangle = \langle\psi_T|\psi(T)\rangle |\psi_T\rangle + P_e |\psi(T)\rangle, \quad (15)$$

with the target state  $|\psi_T\rangle$ , *i.e.* the ground state of  $H_F$ , and the projector  $P_e$  onto the space spanned by the excited states of  $H_F$ .

The expectation value of  $H_F$  with respect to  $|\psi(T)\rangle$  is

$$\langle\psi(T)|H_F|\psi(T)\rangle = |\langle\psi_T|\psi(T)\rangle|^2 E_0 + \langle\phi|H_F|\phi\rangle, \quad (16)$$

with  $|\phi\rangle = P_e |\psi(T)\rangle$  and the ground state energy  $E_0$  of  $H_F$ . The norm of the vector  $|\phi\rangle$  is given in terms of the state fidelity  $F = |\langle\psi_T|\psi(T)\rangle|^2$  via the relation

$$\langle\phi|\phi\rangle = 1 - F. \quad (17)$$

With the inequality

$$\frac{\langle\phi|H_F|\phi\rangle}{\langle\phi|\phi\rangle} \geq E_1, \quad (18)$$

in terms of the energy  $E_1$  of the first excited state of  $H_F$ , the state fidelity is bounded by

$$1 - F \leq \frac{\langle\psi(T)|H_F|\psi(T)\rangle - E_0}{E_1 - E_0}. \quad (19)$$

In order to be evaluable without exponential effort, it is essential that the state vector  $|\psi(T)\rangle$  does not need to be constructed explicitly; but since the expectation values  $\langle\psi(T)|Q|\psi(T)\rangle$  can be constructed with the initial state  $|\Psi(0)\rangle$  and a time-evolved operator  $Q(T)$ , no such state construction is necessary. The propagation of  $Q(t)$  follows Eq. (8), and is thus not impeded by the exponential growth of the Hilbert space. As long as expectation values with respect to the initial state  $|\Psi(0)\rangle$  can be specified efficiently, as it is typically the case in problems of state preparation, adiabatic quantum computation or quantum approximate optimization algorithms [37–39], the state fidelity  $F$  can be bounded efficiently by Eq. (19).

### III. DIABATIC STATE TRANSFER IN A DRIVEN SPIN CHAIN

The approach outlined in Sec. II above is applicable to any set of operators satisfying Eq. (5). The benefits of this approach depend on the size  $d$  of the resulting set



FIG. 1. Linear spin chain of  $n$  qubits with nearest-neighbor  $XX$  interactions. Single-qubit  $Z$ -driving and  $X$ -driving on the end qubits enables efficient preparation of various quantum states, including GHZ and cluster states, and the realization of effective dynamics with multi-qubit interactions.

$\{\mathfrak{a}_j\}$ . Sec. V provides a list of exemplary spin systems and sets of operators with a size that is polynomial in the number of spins. Since such a list of examples is necessarily a bit technical, the following discussion first illustrates solutions to explicit control problems following the general framework outlined in Sec. II with a linear spin chain.

The utilised system Hamiltonian [40]

$$H(t) = \sum_{j=1}^n f_j(t) Z_j + g \sum_{j=1}^{n-1} X_j X_{j+1} + \sum_{j \in \{1, n\}} h_j(t) X_j \quad (20)$$

contains nearest-neighbor interactions in terms of the Pauli  $X$  operators, and single-spin energies in terms of the Pauli  $Z$  operators and the Pauli  $X$  operators on the end-spins of the chain (see Fig. 1).

Without the single-qubit  $X$ -terms, the Hamiltonian would correspond to the regular Ising model. The parity conservation of the Ising model imposes limits on the achievable control, and the Ising model admits a treatment in terms of free Fermions [41] that helps to overcome the exponential effort required to simulate the system dynamics.

The Hamiltonian  $H(t)$  in Eq. (20), on the other hand, has no conserved quantities for  $g \neq 0$  and general time-dependent functions  $f_j(t)$  and  $h_j(t)$ ; *i.e.*, there is no operator  $A$  (apart from multiples of the identity) that commutes with all operators  $Z_j$ ,  $X_1$ ,  $X_n$  and  $\sum_{j=1}^{n-1} X_j X_{j+1}$  as discussed in more detail in Appendix A.

The Lie algebra generated by nested commutators of the individual terms in the Hamiltonian (Eq. (20)) contains  $d = 2n^2 + 3n + 1$  terms as discussed in Sec. V A, and they are given by

$$Z_i, \quad (21a)$$

with  $i \in [1, n]$ ,

$$X_j Z_{jk} X_{j+k+1}, \quad (21b)$$

$$Y_j Z_{jk} Y_{j+k+1}, \quad (21c)$$

$$X_j Z_{jk} Y_{j+k+1}, \quad (21d)$$

$$Y_j Z_{jk} X_{j+k+1}, \quad (21e)$$

with  $j \in [1, n - k - 1]$ ,  $k \in [0, n - 2]$ , and the short-hand

notation  $Z_{jk} = \prod_{i=1}^k Z_{i+j}$ ,

$$Z_{0j}X_{j+1}, \quad (21f)$$

$$Z_{0j}Y_{j+1}, \quad (21g)$$

$$X_{n-j}Z_{(n-j)j}, \quad (21h)$$

$$Y_{n-j}Z_{(n-j)j}, \quad (21i)$$

with  $j \in [0, n-1]$ , and finally

$$\prod_{i=1}^n Z_i. \quad (21j)$$

The present framework thus reduces a control problem in an exponentially large Hilbert space to a problem in a vector space of quadratic growth. Thanks to the quadratic scaling, it is possible to design optimal control protocols for spin chains of lengths that are inaccessible for approaches based on quantum states. The following examples are motivated by typical problems of quantum simulation and state preparation or stabilisation, and they exploit the fact that the Lie algebra given in Eq. (21) contains three-body interactions such as  $X_j Z_{j+1} X_{j+2}$  or even  $n$ -body interactions that cannot be realised by static means.

### A. Target Hamiltonians

Following the discussion of Sec. II C 1, one can seek to find time-dependent functions  $f_j(t)$  and  $h_j(t)$  in the system Hamiltonian  $H(t)$  (Eq. (20)), such that the system initialized in the ground-state of a non-interacting Hamiltonian evolves towards the ground-state of a Hamiltonian with interactions.

A natural choice of non-interacting Hamiltonian based on Eq. (20) is given by the initial conditions  $f_j(0) = f_k(0)$  for all  $j, k$ ,  $f_j(0) \gg g$  and  $h(0) = 0$ , *i.e.* non-interacting spins with single-spin-Z Hamiltonian.

As interacting Hamiltonians defining target states, the subsequent discussion encompasses the Hamiltonian

$$H_G = - \sum_{j=1}^{n-1} X_j X_{j+1} - \prod_{i=1}^n Z_i, \quad (22)$$

whose ground state is a GHZ state, which holds significant importance in the fields of quantum sensing [42], quantum communication [43, 44], and macroscopic quantum mechanics [45], attracting great experimental interest [46, 47]. Another interesting example is the Hamiltonian

$$H_C = Z_1 X_2 + \sum_{j=1}^{n-2} X_j Z_{j+1} X_{j+2} + X_{n-1} Z_n, \quad (23)$$

whose ground state is the one-dimensional  $n$ -qubit cluster state for measurement-based quantum computation [48].

Since the Hamiltonians  $H_G$  and  $H_C$  admit an analytic construction of a target invariant, the following discussion includes also the example

$$H_D = H_C + \sum_{j=1}^{n-1} X_j X_{j+1} \quad (24)$$

to demonstrate that no analytic solutions are necessary preconditions for the present approach. In particular, this Hamiltonian has a vanishing gap in the limit  $n \rightarrow \infty$  which rules out optimal control techniques based on matrix product states [14] as practical alternatives.

### B. Control targets

As discussed in Sec. II C 1, a natural choice for the initial condition  $\mathcal{I}(0)$  is given by

$$\mathcal{I}_0 = \sum_j Z_j \quad (25)$$

for the present problem.

The definition of corresponding control target, however requires some care, and it needs to be done separately for the three different control problems defined in terms of the three Hamiltonians  $H_G$ ,  $H_C$  and  $H_D$ .

#### 1. Control target for GHZ-state Hamiltonian

Even though it is generally not possible to define the control target  $\mathcal{I}_T$  in terms of the Hamiltonian whose ground state is supposed to be realized, this is possible in the case of  $H_G$ . Since  $H_G$  can be expressed as

$$H_G = W_G^\dagger \mathcal{I}_0 W_G, \quad (26)$$

with

$$W_G = \left( \prod_{k=1}^{n-1} e^{-i\frac{\pi}{4}(X_k Y_{k+1})} \right) e^{i\frac{\pi}{4}(X_1 - X_n)}, \quad (27)$$

where the factors in the product are in increasing order in the index  $k$ , the two operators  $H_G$  and  $\mathcal{I}_0$  have the same spectrum; and since every factor in  $W_G$  is induced by elements of the Lie Algebra (Eq. (21)), the unitary  $W_G$  can indeed be realized with the Hamiltonian  $H(t)$  in Eq. (20). The control target  $\mathcal{I}_G = H_G$  is thus a valid choice for the task of realising the ground state of  $H_G$ .

#### 2. Control target for cluster-state Hamiltonian

The construction of control target  $\mathcal{I}_C$  for the task of realising the ground state of  $H_C$  is very similar to the case of  $H_G$  above.

$H_C$  can be expressed as

$$H_C = W_C^\dagger \mathcal{I}_0 W_C \quad (28)$$

with

$$W_C = \left( \prod_{k=1}^{n-1} e^{(-1)^k i \frac{\pi}{4} (X_k X_{k+1})} \right) e^{i \frac{\pi}{4} (X_1 + X_n)}. \quad (29)$$

Also here, all the terms in  $W_C$  are induced by elements of the Lie Algebra (Eq. (21)). Since  $W_C$  is unitary, the control target  $\mathcal{I}_C = H_C$  is thus a valid choice for the task of realising the ground state of  $H_C$  starting with the ground state of  $\mathcal{I}_0$ .

### 3. Control target for $H_D$

While control targets could be defined analytically for the control problem of realizing the ground state of  $H_G$  and  $H_C$ , the case of  $H_D$  seems to require a numerical construction.

Propagating  $\mathcal{I}(t)$  according to Eq. (1) yields operators that are naturally reachable with the available dynamics, and choosing a Hamiltonian  $H_a(t)$  with an adiabatically slow time-dependence can help to find an operator  $\mathcal{I}_a(T_a)$  whose ground state is also ground state of  $H_a(T_a)$  at the end of the adiabatic dynamics.

The following example is based on the choice

$$H_a(t) = \left(1 - \frac{t}{T_a}\right) H_0 + \frac{t}{T_a} H_D + \frac{t}{T_a} \left(1 - \frac{t}{T_a}\right) H_B, \quad (30)$$

where the last term with

$$H_B = \sum_j Z_j + \sum_{j=1}^{n-1} X_j X_{j+1} + X_1 + X_n \quad (31)$$

vanishes at the initial and final point in time ( $t = 0$  and  $t = T_a$ ), but turns some level crossings into avoided crossings, so that adiabatic dynamics does indeed ensure ground-state-to-ground-state transfer.

A control target  $\mathcal{I}_T = \mathcal{I}_a(T_a)$  can be constructed numerically with the adiabaticity parameter  $T_a$  sufficiently large. Since any numerical propagation is based on Eq. (8), the numerical effort follows the quadratic scaling of the Lie algebra (Eq. (21)) and not the exponential scaling of the Hilbert space.

Once the control target is defined, it can be used to construct a time-dependent Hamiltonian that achieves the state transfer in a diabatic fashion.

## C. Results – State transfer

Fig. 2a depicts the infidelity  $\mathcal{J}$  (Eq. (12)) obtained with numerically optimized, time-dependent Hamiltonians as function of the number  $n$  of spins in a chain with

$n$  ranging from 5 to 50. The different solid symbols correspond to the three different target operators discussed in Sec. III A, namely  $H_G$  (Eq. (22)) (red diamonds),  $H_C$  (Eq. (23)) (blue squares) and  $H_D$  (Eq. (24)) (black triangles). The optimisations for  $H_G$  and  $H_C$  are intentionally terminated when infidelities below  $10^{-6}$  are reached. The operator  $H_D$ , however has a vanishing gap in the limit  $n \rightarrow \infty$ , and the closing gap requires longer running time; in the case of  $H_D$ , the optimisation is thus terminated once a maximum number of iterations, around  $10^3$ , is reached.

The empty red diamonds and blue squares depict the bound of Eq. (19) on the state fidelity for the ground states of  $H_G$  and  $H_C$ . The closing gap of  $H_D$  on the other hand makes this bound unsuited for  $H_D$ . The state fidelity in this case is thus estimated from numerical propagations with matrix product states [49, 50] for qubit numbers  $n \leq 30$ , as depicted by the empty triangles in Fig. 2a. Despite the efficient matrix-product representation of the initial and final states, the states at in-between times created by the controlled dynamics for  $n \geq 35$  require bond dimensions exceeding 500, rendering numerical optimisation impractical.

In all three cases shown in cases Fig. 2a, the achieved state fidelities confirm successful optimal control for system sizes far outside the regime accessible to explicit state control. In particular, the state infidelities are all well below the limits imposed by system imperfections of current or foreseeable quantum devices [51].

Interestingly, because of the constant interaction term in the system Hamiltonian (Eq. (20)) there is a minimal time required for the state transfer, also referred to as quantum speed limit [52]. In order to obtain infidelities as low as in Fig. 2, the duration of the controlled dynamics needs to increase with the system size, but a modest approximately linear increase ( $T \sim n\pi/2g$ ) with the qubit number  $n$ , and the timescale  $1/g$  defined by the interaction constant  $g$  in Eq.(20) is sufficient for the ground state transfer.

## IV. REALIZATION OF PROPAGATORS

As sketched in Sec. II C 2, the current approach can also be used to construct a time-dependent Hamiltonian to induce dynamics that coincides with a desired unitary  $U_T$  at a given time  $T$ . This is exemplified here in more detail for  $U_T = \exp(-i\pi/8 H_T)$  with  $H_T$  given by the three Hamiltonians  $H_G$  (Eq. (22)),  $H_C$  (Eq. (23)) and  $H_D$  (Eq. (24)), and system dynamics in terms of the Hamiltonian  $H(t)$  in Eq. (20).

### A. Objective function

The crucial question that will ultimately determine the required numerical effort is how many (and which) initial conditions  $\mathcal{I}_j(0)$  for the infidelity  $\mathcal{J}_{U_T}$  in Eq. (14) need

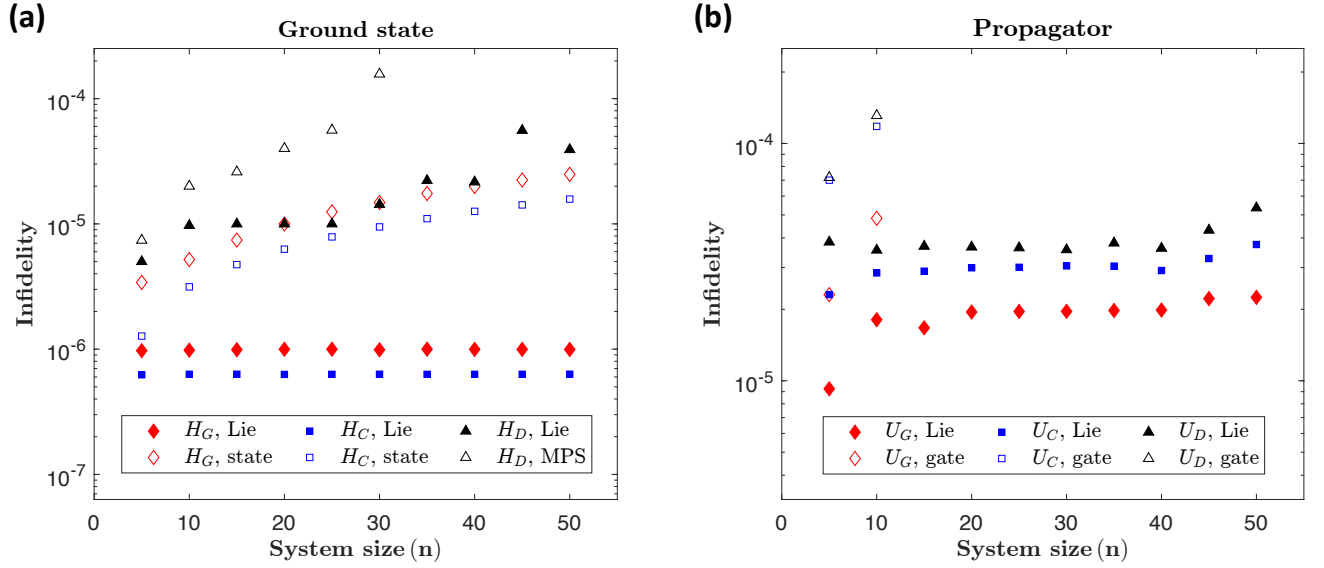


FIG. 2. Infidelity for dynamics for a spin chain (Eq. (20)) with optimized single-qubit driving, as function of systems size  $n$ . Solid shapes depict infidelities  $\mathcal{I}$  (Eq. (12)) in log-scale for state transfer (panel a) and infidelities  $\mathcal{I}_{U_T}$  (Eq. (14)) for quantum gates (panel b). Empty diamonds and squares in panel a depict bounds (Eq. (19)) on state infidelities; empty triangles in panel a represent state infidelities and empty shapes in panel b depict gate infidelities. As result of the optimization, the values of the infidelities  $\mathcal{I}$  and  $\mathcal{I}_{U_T}$  are largely independent of the system size  $n$ . Actual state- and gate-infidelities do grow with increasing system size, but they remain well below what can be achieved given the experimental imperfections of actual quantum devices.

to be considered in order to obtain a faithful objective function.

With the initial conditions

$$\mathcal{I}_j(0) = Z_j, \quad (32a)$$

for  $j \in [1, n]$ ,

$$\mathcal{I}_{j+n}(0) = X_j X_{j+1}, \quad (32b)$$

for  $j \in [1, n-1]$ , and

$$\mathcal{I}_{2n}(0) = X_1 + X_n, \quad (32c)$$

the infidelity  $\mathcal{I}_{U_T}$  in Eq. (14) vanishes exactly for the target gate  $U_T$  in Eq. (14) for any target that is reachable with  $H(t)$  in Eq. (20). That is to say that the relation  $U\mathcal{I}_j(0)U^\dagger = U_T\mathcal{I}_j(0)U_T^\dagger$  can be simultaneously satisfied for all these choices  $\mathcal{I}_j(0)$  only if  $U = U_T \exp(i\varphi)$ , where  $\exp(i\varphi)$  is a global phase factor.

To see that this is indeed the case, it is helpful to notice that the set of relations  $U\mathcal{I}_j(0)U^\dagger = U_T\mathcal{I}_j(0)U_T^\dagger$  is equivalent to the set of commutation relations

$$[U_T^\dagger U, \mathcal{I}_j(0)] = 0. \quad (33)$$

As shown in Sec. A, the only operators that commute with each of the operators in Eq. (32) are multiples of the identity, which leaves  $U_T^\dagger U = \exp(i\varphi)\mathbb{1}$  as the only solution.

While this provides a faithful objective function, its use in an optimisation implies the evaluation of  $2n$  summands in Eq. (14) at any step in the optimisation. For

the sake of efficiency, it can be preferable to use the objective functional  $\mathcal{I}_{U_T}$  with only five initial conditions

$$\mathcal{I}_1(0) = \sum_k Z_{2k+1}, \quad (34a)$$

$$\mathcal{I}_2(0) = \sum_k Z_{2k}, \quad (34b)$$

$$\mathcal{I}_3(0) = \sum_k X_{2k+1} X_{2k+2}, \quad (34c)$$

$$\mathcal{I}_4(0) = \sum_k X_{2k} X_{2k+1}, \quad (34d)$$

$$\mathcal{I}_5(0) = X_1 + X_n. \quad (34e)$$

Even though the optimal value can be obtained for propagators different than  $U_T$ , optimizations do not seem to converge to such a solution in practice. Since verification requires only a single propagation, it is numerically advantageous to use this objective function (with Eqs. (34) as initial conditions) for the optimisation, and eventually use the faithful objective function (with Eqs. (32) as initial conditions) only for verification of the final solution.

## B. Results – Propagators

Fig. 2b depicts the infidelities  $\mathcal{I}_{U_T}$  defined in Eq. (14) together with Eq. (32) for optimized Hamiltonian as function of system size  $n$  with solid red diamonds for

$U_T = \exp(-i\pi/8 H_G)$ , solid blue squares for  $U_T = \exp(-i\pi/8 H_C)$  and solid black triangles for  $U_T = \exp(-i\pi/8 H_D)$ .

The empty shapes in the figure show actual gate infidelities,  $1 - |\text{tr}(U^\dagger(T)U_T)|^2 / 2^{2n}$ , obtained with numerically exact integration of the Schrödinger equation. Since this type of verification is limited by the exponential scaling of the Hilbert space, actual gate infidelities are shown for up to  $n = 10$  only. Within what is numerically achievable, the gate infidelities do confirm the success of the control protocols designed with the present framework, and similarly to the task of state preparation, the realisation of desired propagators is achieved with infidelities far below of what could be experimentally resolved with existing technology [5, 53].

Also the duration of controlled dynamics required for the realization of a desired propagator, has a fundamental limit given by the interaction strength  $g$ . The numerically observed minimal time required to implement the unitaries induced by  $H_C$  and  $H_D$  is independent of the system size ( $\sim \pi/2g$ ), but the minimal time required to implement the unitary induced by  $H_G$  scales linearly in the number of qubits ( $\sim 2n\pi/g$ ). Given that  $H_C$  and  $H_D$  contain at most three-body interactions, whereas  $H_G$  contains an  $n$ -body interaction, *i.e.* an interaction whose type changes with increasing system size  $n$ , the numerically observed dependence of minimal durations of controlled dynamics seem consistent with the underlying problem, which generates some confidence that the obtained solutions are close to the actual global solution of the control problem.

## V. MORE SETS OF OPERATORS WITH POLYNOMIAL SCALING

While the discussion in Secs. III and IV is meant to exemplify the use of the current approach for actual control problems, a similarly detailed discussion for further examples would be repetitive. The goal of this section is thus to provide further insight into sets of operators for which the present approach provides an advantage over treatments in terms of state vectors. In the following, a few exemplary algebras with polynomial scaling are provided for different interaction geometries. The corresponding commutation relations are available at [54].

### A. Spin chain

The Lie algebra specified in Eq. (21) is generated by the terms

$$\mathfrak{h}_j = Z_j , \quad (35a)$$

with  $j \in [1, n]$ ,

$$\mathfrak{h}_{j+n} = X_j X_{j+1} , \quad (35b)$$

with  $j \in [1, n-1]$ , and

$$\mathfrak{h}_{2n} = X_1 , \quad (35c)$$

$$\mathfrak{h}_{2n+1} = X_n . \quad (35d)$$

Commutators between terms in Eq. (35a) and terms in Eq. (35b) yield operators of the form  $X_j Y_{j+1}$  and  $Y_j X_{j+1}$ , and commutators between those and terms in Eq. (35a) yields operators of the form  $Y_j Y_{j+1}$ . The Lie algebra thus contain the terms

$$X_j X_{j+1} , X_j Y_{j+1} , Y_j X_{j+1} , Y_j Y_{j+1} . \quad (36)$$

Commutators between such terms yield operators of the form  $A_j Z_{j+1} B_{j+2}$  (with  $A$  and  $B \in \{X, Y\}$ ), and nested commutators with several terms of Eq. (36) yield operators of the form

$$A_j Z_{j+1} \dots Z_{j+k} B_{j+k+1} . \quad (37)$$

Commutators between these  $k+2$ -body interactions and the terms  $X_1$  and  $X_n$  (Eqs. (35c) and (35d)) yields the terms

$$Z_1 \dots Z_l A_{l+1} , \quad (38a)$$

$$A_{n-l} Z_{n-l+1} \dots Z_n , \quad (38b)$$

and

$$Z_1 \dots Z_n . \quad (38c)$$

Those are exactly the terms specified in Eq. (21), and they do indeed form a closed Lie algebra.

With  $n$  terms in Eq. (35a),  $2n(n-1)$  terms in Eq. (37) (that include Eq. (35b) and Eq. (36) as special cases),  $2n-1$  terms from Eqs. (38a) and (38b) each, as well as one term in Eqs. (35c), Eqs. (35d) and (38c) respectively, the total number of elements in the Lie algebra is  $d = 2n^2 + 3n + 1$ .

### B. Driven spin comb

An interaction geometry that results in a Lie algebra of quadratic size in the qubit number  $n$  that can be used to realize elementary building blocks of topologically protected quantum information processing [55] is depicted in Fig. 3(a). It is a comb-structure with a linear chain of  $m = n/2$  qubits with nearest-neighbour interactions, and a second chain of another  $m$  qubits interacting only with qubits on the first chain.

Because of this geometry, each Pauli operator carries two indices. The first (lower) index specifies the position of the qubit within its chain, and the second (upper) index identifies the chain itself (1 for the top chain and 2 for the bottom chain).

The elementary Hamiltonian terms  $\mathfrak{h}_i$  (for the definition of a system Hamiltonian in Eq. (3)) are given by

$$\mathfrak{h}_j = Z_j^1 Z_j^2 , \quad (39a)$$



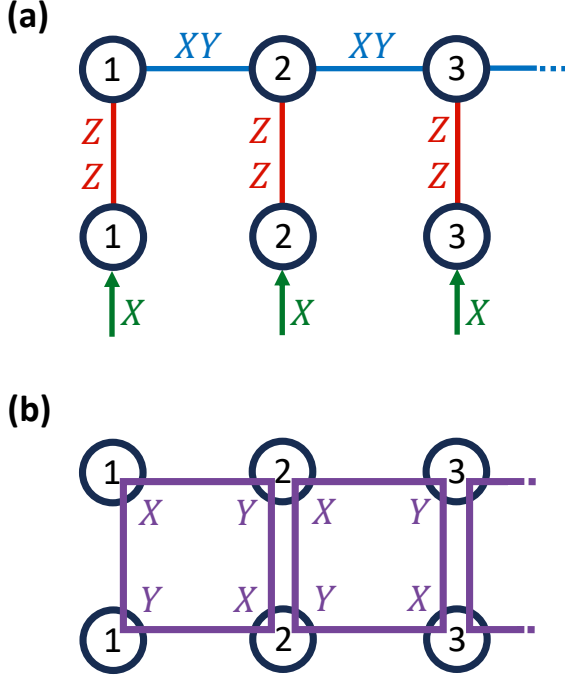


FIG. 3. Spin comb with nearest-neighbour  $XY$  interactions in the top chain and  $ZZ$  interactions between spins of different chains (inset (a)). Single-spin  $X$ -driving (inset (a)) enables the realization of effective dynamics with four-spin interactions matching the Toric Code Plaquette operators Eq. (42) (inset (b)).

with  $j \in [1, m]$ ,

$$\mathfrak{h}_{j+m} = X_j^2, \quad (39b)$$

with  $j \in [1, m]$ , and

$$\mathfrak{h}_{j+2m} = X_j^1 Y_{j+1}^1, \quad (39c)$$

with  $j \in [1, m-1]$ .

In order to understand the Lie algebra generated by Eqs. (39), and, in particular its scaling with  $m$ , it is instructive to start with the Lie algebra generated by the terms in Eq. (39c) only. The terms in Eq. (39c) form a subset of the terms in Eq. (36), and similarly to the discussion in Sec. V A the resultant Lie algebra is comprised of the terms

$$X_j^1 Z_{jk} Y_{j+k+1}^1, \quad (40)$$

with  $j+k+1 \leq m$  and the short-hand notation  $Z_{jk} = \prod_{i=1}^k Z_{i+j}^1$ .

Commutation between the terms in Eq. (40) and the terms in Eq. (39a) yields the terms

$$Y_j^1 Z_{jk} Y_{j+k+1}^1 Z_j^2, \quad (41a)$$

$$X_j^1 Z_{jk} X_{j+k+1}^1 Z_{j+k+1}^2, \quad (41b)$$

$$Y_j^1 Z_{jk} X_{j+k+1}^1 Z_j^2 Z_{j+k+1}^2. \quad (41c)$$

With  $m(m-1)/2$  terms in Eq. (40) (that includes the elements in Eq. (39c)), 3 terms in Eq. (41), and  $m$  elements in Eq. (39a), the Lie algebra generated by the terms in Eq. (39a) and Eq. (39c) thus contain  $2m^2 - m$  terms.

Commutation with the terms in Eq. (39b) yields terms of similar structure to the terms in Eq. (41), but with operators  $Z_j^2$  and/or  $Z_{j+k+1}^2$  replaced by the corresponding operator of  $X$  or  $Y$  type. The number of operators of the type in Eqs. (41a) and (41b) is thus increased by a factor of 3, and the number of operators of the type in Eq. (41c) is increased by a factor of 9. The Lie algebra generated by all the terms in Eq. (39) thus has  $3m(3m-1)/2$  terms.

Within this Lie algebra are terms of the form

$$Q_j = X_j^1 Y_{j+1}^1 Y_j^2 X_{j+1}^2, \quad (42)$$

corresponding to a four-body interaction on four spins forming a square as depicted in Fig. 3(b). The operators  $Q_j$  and  $Q_{j+1}$  act on two different quartets of spins with an overlap on two spins (with index  $j+1$ ). The factor of  $Q_j$  on these spins is given by  $Y_{j+1}^1 X_{j+1}^2$ , and the factor of  $Q_{j+1}$  on these spins is given by  $X_{j+1}^1 Y_{j+1}^2$ . All the operators  $Q_j$  are thus mutually commuting, even though their single-spin factors on overlapping spins are not mutually commuting. The present example is thus suitable for the realization of a ribbon of plaquette operators of the toric code [23].

### C. Hexagonal spin ladder

Fig. 4 depicts a spin-ladder with hexagonal structures, similar the Kitaev honeycomb model [23], but with the two interactions of the spin at the bottom of each hexagon commuting with each other. This interaction geometry results in a Lie-algebra of dimension  $(25n^2 - 40n + 12)/32$  with  $n = 4n_h + 2$  spins, where  $n_h$  is the number of hexagons. In contrast, the interaction geometry of the original Kitaev honeycomb model scales exponentially  $(2^{n_h} n (n-1)/2)$ .

The individual operators  $\mathfrak{h}_j$  entering the system Hamiltonian read

$$\mathfrak{h}_j = Y_{2j-1}^1 Y_{2j}^1, \quad (43a)$$

$$\mathfrak{h}_{j+(m-1)/2} = Z_{2j}^1 Z_{2j+1}^1, \quad (43b)$$

$$\mathfrak{h}_{j+m-1} = X_{2j}^2 X_{2j+1}^2, \quad (43c)$$

$$\mathfrak{h}_{j+(3m-3)/2} = Z_{2j-1}^2 X_{2j}^2, \quad (43d)$$

$$\mathfrak{h}_{l+2m-2} = X_{2l-1}^1 Y_{2l}^2, \quad (43e)$$

with  $m = n/2$ ,  $j \in [1, (m-1)/2]$ ,  $l \in [1, (m+1)/2]$ . The resultant Lie algebra can be constructed systematically similarly to the discussion in Sec. V A; because of the more intricate interaction geometry the exact form of the individual elements is a bit more bulky, and it is deferred to Appendix C.

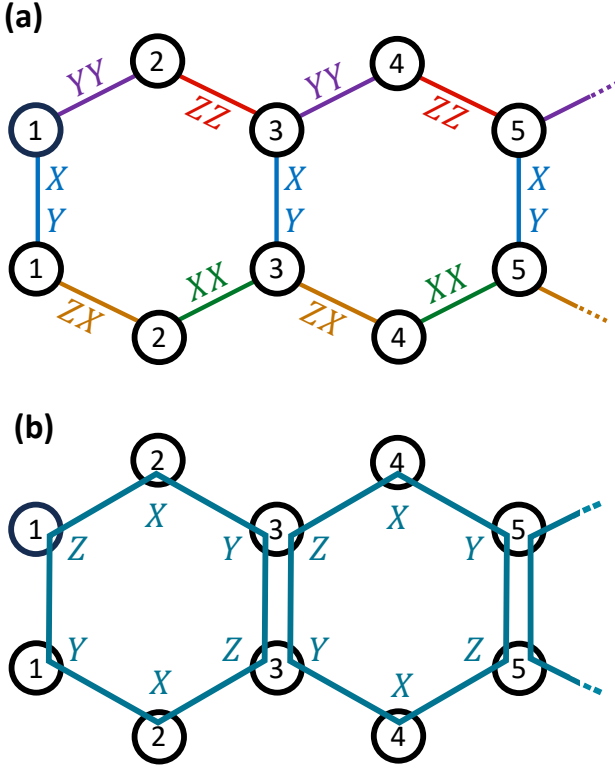


FIG. 4. Spin-ladder with hexagonal structures. Each spin interacts with its nearest neighbours, but in contrast to the Kitaev honeycomb model that includes only mutually non-commuting interactions for any spin, there is one spin (at the bottom of each hexagon) that has two commuting interactions (inset (a)). This interaction geometry results in a Lie algebra of quadratic size with elements including the plaquette operators (Eq. (44), inset (b)) that are crucial in the field of topological stabilizer codes.

Crucially, the Lie algebra contains the 6-body plaquette operators

$$P_j = Z_{2j-1}^1 X_{2j}^1 Y_{2j+1}^1 Y_{2j-1}^2 X_{2j}^2 Z_{2j+1}^2, \quad (44)$$

as depicted schematically in Fig. 4b. These operators, that commute with the Kitaev honeycomb Hamiltonian [23], form a central part in the realization of error-correcting surface codes on hexagonal lattices [56, 57]. In particular, plaquette operators together with two-body operators like  $X_{2l-1}^1 Y_{2l-1}^2$ , can form the basis for stabilizer operators, as exemplified by the  $XYZ^2$  topological stabilizer code [58]. The present framework can thus be used to aid the realization of quantum error correction.

## VI. OUTLOOK

While the exponential scaling of composite quantum systems poses fundamental constraints that can not be overcome in general, the fact that there are invariants with favourable scaling does allow us to overcome them

in specific cases. With control over interaction geometries in various platforms such as superconducting qubits [59], trapped ions and Rydberg atoms [60] the present approach can help to fully exploit the qubit count in current devices (ranging up to 256 [60]) without the need of long gate sequences that are conflicting with decoherence and the accumulation of individual gate errors. While verification of the functionality of a quantum device is a challenging problem [61], the description of quantum dynamics in terms of invariants can also be used to make predictions for the targeted dynamics that can be experimentally tested.

With three-body and four-body interactions naturally arising in the dynamics induced by the spin Hamiltonian given in Eq. (20), the present approach can also support the realisation of error correcting codes [62, 63] and topologically protected quantum information processing [55]. With the advent of highly controllable systems that pose control problems beyond the limitations of classical simulations [60], there is a growing need for control techniques with good scaling behaviour. Optimisations with the present framework can help to avoid or support costly experimental optimisations [46, 64]. The resulting ability to create quantum states that allow for sensing at the Heisenberg limit makes the present approach a valuable tool for the community's effort towards the development of quantum technological applications.

## Acknowledgements

This work was supported by the U.K. Engineering and Physical Sciences Research Council via the EPSRC Hub in Quantum Computing and Simulation (EP/T001062/1) and the UK Innovate UK (project number 10004857). We are indebted to stimulating discussions with Leonardo Bianchi, Man Hei Cheng and Oliver Reardon-Smith. The optimised pulse and computer code for this work are available without restriction [54].

M.O.-R. and N.H.L contributed equally to this work.

## Appendix A: Absence of Symmetries in the Control Hamiltonian

We will show here that there is no symmetry in the Hamiltonian

$$H(t) = \sum_{j=1}^n f_j(t) Z_j + g \sum_{j=1}^{n-1} X_j X_{j+1} + \sum_{j \in \{1, n\}} h_j(t) X_j \quad (A1)$$

for  $g \neq 0$  and general time-dependent functions  $f_j(t)$  and  $h_j(t)$ , *i.e.*

there is no  $n$ -qubit operator  $A^n$  (besides multiples of the identity) that commutes with each of the operators  $Z_1, Z_2, \dots, Z_n, X_1, X_n$  and  $\sum_{j=1}^n X_j X_{j+1}$ .

The requirement to commute with each of the operators  $Z_1, Z_2, \dots, Z_n$  implies that  $A^n$  can be expanded in terms of tensor-products of  $\mathbb{1}$  and  $Z$  terms only.

The requirement to also commute with  $X_1$  and  $X_n$  then implies that  $A^n$  is of the form

$$A^n = \mathbb{1} \otimes D^n \otimes \mathbb{1}, \quad (\text{A2})$$

with an  $n - 2$ -qubit operator  $D^n$  that can be expanded in terms of tensor-products of  $\mathbb{1}$  and  $Z$  terms, or, more explicitly as

$$A^n = \mathbb{1}_1 \otimes F^n \otimes \mathbb{1}_{n-1} \otimes \mathbb{1}_n + \mathbb{1}_1 \otimes G^n \otimes Z_{n-1} \otimes \mathbb{1}_n, \quad (\text{A3})$$

with  $n - 3$ -qubit operators  $F_n$  and  $G_n$  that can be expanded in terms of tensor-products of  $\mathbb{1}$  and  $Z$  terms,

In order to address commutativity with

$$\sum_{j=1}^{n-1} X_j X_{j+1} = H_x^n, \quad (\text{A4})$$

it is instructive to express  $H_x^n$  as

$$H_x^n = H_x^{n-1} \otimes \mathbb{1}_n + \mathbb{1}_{1\dots n-1} \otimes X_{n-1} \otimes X_n. \quad (\text{A5})$$

The commutator  $[A^n, H_x^n]$  thus reads

$$[A^n, H_x^n] = [\mathbb{1}_1 \otimes G^n \otimes Z_{n-1}, H_x^{n-1}] \otimes \mathbb{1}_n \quad (\text{A6})$$

$$+ 2i \mathbb{1}_1 \otimes G^n \otimes Y_{n-1} \otimes X_n \quad (\text{A7})$$

$$+ [\mathbb{1}_1 \otimes F^n \otimes \mathbb{1}_{n-1}, H_x^{n-1}] \otimes \mathbb{1}_n. \quad (\text{A8})$$

Since the term in (A7) is the only term with a factor  $X_n$ , the commutator can vanish only if  $G^n$  vanishes. If this is the case, however, then also the right-hand-side in (A6) vanishes, such that the commutator reduces to

$$[A^n, H_x^n] = [\mathbb{1}_1 \otimes F^n \otimes \mathbb{1}_{n-1}, H_x^{n-1}] \otimes \mathbb{1}_n, \quad (\text{A9})$$

with an operator

$$A^{n-1} = \mathbb{1}_1 \otimes F^n \otimes \mathbb{1}_{n-1}, \quad (\text{A10})$$

that is exactly of the form of Eq. (A2), but for  $n - 1$  instead of  $n$  qubits.

The result to be proven thus holds for an  $n$ -qubit system, provided that it holds for an  $n - 1$  qubits system, and since one can readily verify it explicitly for a 2 qubits system, the proof is completed by induction.

## Appendix B: Numerical optimisation

This section describes the numerical techniques used to find the optimal control strategies for state transfer and propagator realization problems, as detailed in Secs. III and IV. The optimal solutions minimize a fidelity measure (defined in Eq. (12) for state transfer and in Eq. (14) for propagator realization) by finding a suitable time dependence of the control Hamiltonian in Eq. (20).

Piece-wise control is utilized in the control Hamiltonian, dividing the pulse duration  $T$  into  $M$  intervals with constant driving amplitude in each interval. The optimization process aims to minimize the infidelity (Eq. (12) or Eq. (14)) by optimizing the set of control amplitudes  $\{f_j^l, h_1^l, h_n^l : 1 \leq l \leq M, 1 \leq j \leq n\}$  and the total duration  $T$ . To efficiently evaluate the infidelity during optimization, the operator basis elements  $\{\mathbf{a}_j\}$  are normalized, *i.e.* satisfy  $\text{tr}(\mathbf{a}_j \mathbf{a}_k) = \delta_{jk}$ . This normalization simplifies the propagation of operators according to Eq. (8) and the subsequent calculation of the overlap between the target coefficient vector  $\mathbf{a}_T$  and the final coefficient vector  $\mathbf{a}(T)$  obtained from an initial condition  $\mathbf{a}(0)$ .

The evolution of  $\mathbf{a}(t)$  is obtained with a Krylov subspace method to take advantage of the sparsity of  $K(t)$ . We feed the infidelity and its gradient with respect to the control variables to a gradient-based optimisation algorithm. The interior point method is employed, and the Hessian is approximated with the L-BFGS method. This algorithm is implemented in the `fmincon` function in Matlab.

For large  $n$ , there are many shallow local minima and plateaus in the control landscape, especially for  $U_G$  due to the difficulty of reaching the  $n$ -body interaction term. To systematically address these challenges, a three-step procedure is employed. Initially, the symmetry of the control problem is imposed on the control variables, followed by the relaxation of this symmetry. Specifically, we begin with

$$H_1^c(t) = g \sum_{j=1}^{n-1} X_j X_{j+1} + f_1(t) \sum_{j=1}^n Z_j + f_2(t)(Z_1 + Z_n) + h(t)(X_1 + X_n), \quad (\text{B1})$$

which is a translationally invariant control, except at the two ends, *i.e.*, it has the same symmetry as the control targets. The optimisation is done sequentially from  $n = 5$  to  $n = 50$  in step of 5 where the optimal control for  $n - 5$  is used as the initial guess for  $n$ .

We then lower the infidelity for each  $n$  by optimising with a control Hamiltonian with inversion symmetry

$$H_2^c(t) = g \sum_{j=1}^{n-1} X_j X_{j+1} + \sum_{j=1}^{\lfloor (n+1)/2 \rfloor} f_j(t)(Z_j + Z_{n+1-j}) + h(t)(X_1 + X_n), \quad (\text{B2})$$

using the final control in the previous step as the initial guess. Finally, we refine the solution further by optimizing with a control Hamiltonian that lacks any symmetry

$$H_3^c(t) = g \sum_{j=1}^{n-1} X_j X_{j+1} + \sum_{j=1}^n f_j(t) Z_j + \sum_{j \in \{1, n\}} h_j(t) X_j. \quad (\text{B3})$$

Each optimisation step is done with a maximum of 1000 function-and-gradient evaluations. At every step, small

random perturbations are applied to the initial guess to explore 12 nearby solutions in parallel, facilitating escape from traps. In many cases the threshold infidelity is reached already with  $H_1^c(t)$  or  $H_2^c(t)$ .

For the optimisations of  $H_C, H_D, H_G, T \approx n\pi/2g$  and the number of time bins in the piece-wise control pulse is  $M = 10n$ . For  $U_C$  and  $U_D, T \approx \pi/2g$  and  $M = 10n$ . For  $U_G, T \approx 2n\pi/g$  and  $M = 20n$ .

The state infidelity for  $H_D$  in Fig. 2 was obtained with MPS. The ground state of  $H_D$  is computed with DMRG, and the final state is obtained by evolving the initial state  $|\psi_0\rangle$  with the MPO (matrix product operator)  $W^{II}$  method [50], where each time bin is further divided into 20 smaller steps to reduce error. All MPS calculations are done using the Tenpy package [49].

### Appendix C: Lie algebra of the hexagonal spin ladder

As shown in the following, the Lie algebra generated by the operators in Eq. (43) for the spin ladder depicted in Fig. 4 scales as  $(25n^2 - 40n + 12)/32$  in the number of spins  $n = 4n_h + 2$  with  $n_h$  hexagons.

In order to arrive at this scaling, it is convenient to start with two non-interacting chains.

The Lie algebra for the top chain is generated by Eqs. (43a) and (43b). With the short-hand notation  $X_{jk} = \prod_{i=1}^k X_{i+j}^1$ , and

$$\overline{Y}Z_{jk} = Y_j^1 X_{jk} Z_{j+k+1}^1, \quad (\text{C1a})$$

$$\overline{Z}Y_{jk} = Z_j^1 X_{jk} Y_{j+k+1}^1, \quad (\text{C1b})$$

$$\overline{Y}Y_{jk} = Y_j^1 X_{jk} Y_{j+k+1}^1, \quad (\text{C1c})$$

$$\overline{Z}Z_{jk} = Z_j^1 X_{jk} Z_{j+k+1}^1, \quad (\text{C1d})$$

it is given by the operators  $\gamma_{jk}$  with  $j \in [1, m-1]$  and  $k \in [0, m-j-1]$ , where

$$\gamma_{jk} = \begin{cases} \overline{Y}Z_{jk}, & \text{for odd } j \text{ and odd } k, \\ \overline{Y}Y_{jk}, & \text{for odd } j \text{ and even } k, \\ \overline{Z}Y_{jk}, & \text{for even } j \text{ and odd } k, \\ \overline{Z}Z_{jk}, & \text{for even } j \text{ and even } k. \end{cases} \quad (\text{C2})$$

The Lie algebra for the bottom chain is generated by Eqs. (43c) and (43d), and it includes (besides Eqs. (43c) and (43d))

$$X_{2j}^2 Y_{2j+1}^2 X_{2j+2}^2, \quad (\text{C3})$$

with  $j \in [1, (m-3)/2]$ .

With  $s \in \{-1, 1\}$ ,  $j \in [1, (m-1)/2]$ ,  $k \in [0, m-j-1]$ , and with  $\Gamma_{2j}$  adopting the four different values

$$\Gamma_{2j} = \begin{cases} X_{2j-1}^2 X_{2j}^2, \\ Y_{2j-1}^2 \mathbb{1}_{2j}^2, \end{cases} \quad (\text{C4})$$

for  $s = -1$ ,

$$\Gamma_{2j} = \begin{cases} X_{2j}^2 Z_{2j+1}^2, \\ \mathbb{1}_{2j}^2 Y_{2j+1}^2, \end{cases} \quad (\text{C5})$$

for  $s = 1$ , the Lie algebra generated by the full set of operators in Eq. (43) contains the additional terms

$$X_{2j+s}^1 \Gamma_{2j}, \quad (\text{C6a})$$

$$\overline{Z}Y_{2j+s,k} \Gamma_{2j}, \quad (\text{C6b})$$

$$\overline{Z}Y_{2j-1-k+s,k} \Gamma_{2j}, \quad (\text{C6c})$$

for even  $k$ , and

$$\overline{Z}Z_{2j+s,k} \Gamma_{2j}, \quad (\text{C6d})$$

$$\overline{Z}Y_{2j+s,k} \Gamma_{2j} Y_{2j+k+s+1}^2, \quad (\text{C6e})$$

$$\overline{Z}Y_{2j+s,k} \Gamma_{2j} X_{2j+k+s}^2 Z_{2j+k+s+1}^2, \quad (\text{C6f})$$

$$\overline{Z}Y_{2j+s,k} \Gamma_{2j} X_{2j+k+s+1}^2 Z_{2j+k+s+2}^2, \quad (\text{C6g})$$

$$\overline{Y}Y_{2j-1-k+s,k} \Gamma_{2j}, \quad (\text{C6h})$$

$$\overline{Z}Y_{2j-1-k+s,k} Y_{2j-1-k+s}^2 \Gamma_{2j}, \quad (\text{C6i})$$

$$\overline{Z}Y_{2j-1-k+s,k} X_{2j-2-k+s}^2 Z_{2j-1-k+s}^2 \Gamma_{2j}, \quad (\text{C6j})$$

$$\overline{Z}Y_{2j-1-k+s,k} X_{2j-1-k+s}^2 X_{2j-k+s}^2 \Gamma_{2j}, \quad (\text{C6k})$$

for odd  $k$ .

Given that Eqs. (43c)-(43d) contain  $(n-2)/2$  elements, Eq. (C2) includes  $(n^2/8 - n/4)$  elements (encompassing Eqs. (43a) and (43b)), Eq. (C3) contributes with  $(n-6)/4$  elements, and Eq. (C6) adds  $(21n^2 - 56n + 92)/32$  operators, the size of the Lie algebra grows as  $(25n^2 - 40n + 12)/32$  with the number of qubits  $n = 2 + 4n_h$  defined in terms of the number of hexagons  $n_h$ .

For  $k = 1$ ,  $s = 1$  and  $\Gamma_{2j} = X_{2j}^2 Z_{2j+1}^2$ , the operator in Eq. (C6i) reduces to the 6-body plaquette operators  $P_j = Z_{2j-1}^1 X_{2j}^1 Y_{2j+1}^1 Y_{2j-1}^2 X_{2j}^2 Z_{2j+1}^2$  in Eq. (44).

- 
- [1] T. H. Johnson, S. R. Clark, and D. Jaksch, What is a quantum simulator?, EPJ Quantum Technology **1**, <https://doi.org/10.1140/epjqt10> (2014).  
[2] D. Marcos, P. Rabl, E. Rico, and P. Zoller, Superconducting circuits for quantum simulation of dynamical gauge

- fields, Physical Review Letters **111**, 110504 (2013).  
[3] J. Werschnik and E. Gross, Quantum optimal control theory, Journal of Physics B: Atomic, Molecular and Optical Physics **40**, R175 (2007).  
[4] C. P. Koch, U. Boscain, T. Calarco, G. Dirr, S. Fil-

- ipp, S. J. Glaser, R. Kosloff, S. Montangero, T. Schulte-Herbrüggen, D. Sugny, *et al.*, Quantum optimal control in quantum technologies. strategic report on current status, visions and goals for research in europe, EPJ Quantum Technology **9**, 19 (2022).
- [5] T. D. Ladd, F. Jelezko, R. Laflamme, Y. Nakamura, C. Monroe, and J. L. O'Brien, Quantum computers, Nature **464**, 45 (2010).
- [6] I. Buluta and F. Nori, Quantum simulators, Science **326**, 108 (2009).
- [7] A. Aspuru-Guzik and P. Walther, Photonic quantum simulators, Nature Physics **8**, 285 (2012).
- [8] I. Bloch, J. Dalibard, and S. Nascimbene, Quantum simulations with ultracold quantum gases, Nature Physics **8**, 267 (2012).
- [9] A. Gaita-Ariño, F. Luis, S. Hill, and E. Coronado, Molecular spins for quantum computation, Nature Chemistry **11**, 301 (2019).
- [10] A. J. Daley, I. Bloch, C. Kokail, S. Flannigan, N. Pearson, M. Troyer, and P. Zoller, Practical quantum advantage in quantum simulation, Nature **607**, 667 (2022).
- [11] N. Khaneja, T. Reiss, C. Kehlet, T. Schulte-Herbrüggen, and S. J. Glaser, Optimal control of coupled spin dynamics: design of NMR pulse sequences by gradient ascent algorithms, Journal of Magnetic Resonance **172**, 296 (2005).
- [12] T. Schulte-Herbrüggen, A. Spörl, N. Khaneja, and S. J. Glaser, Optimal control-based efficient synthesis of building blocks of quantum algorithms: A perspective from network complexity towards time complexity, Physical Review A **72**, 042331 (2005).
- [13] W. J. Chetcuti, C. Sanavio, S. Lorenzo, and T. J. G. Apollaro, Perturbative many-body transfer, New Journal of Physics **22**, 033030 (2020).
- [14] P. Doria, T. Calarco, and S. Montangero, Optimal control technique for many-body quantum dynamics, Physical Review Letters **106**, 190501 (2011).
- [15] D. Burgarth, K. Maruyama, M. Murphy, S. Montangero, T. Calarco, F. Nori, and M. B. Plenio, Scalable quantum computation via local control of only two qubits, Physical Review A **81**, 040303 (2010).
- [16] N. H. Le, M. Cykiert, and E. Ginossar, Scalable and robust quantum computing on qubit arrays with fixed coupling, npj Quantum Information **9**, 1 (2023).
- [17] A. Castro, J. Werschnik, and E. K. Gross, Controlling the dynamics of many-electron systems from first principles: A combination of optimal control and time-dependent density-functional theory, Physical Review Letters **109**, 153603 (2012).
- [18] F. Verstraete, V. Murg, and J. I. Cirac, Matrix product states, projected entangled pair states, and variational renormalization group methods for quantum spin systems, Advances in Physics **57**, 143 (2008).
- [19] G. Carleo and M. Troyer, Solving the quantum many-body problem with artificial neural networks, Science **355**, 602 (2017).
- [20] D. Gottesman, *Stabilizer codes and quantum error correction* (California Institute of Technology, 1997).
- [21] R. Raussendorf, D. E. Browne, and H. J. Briegel, Measurement-based quantum computation on cluster states, Physical Review A **68**, 022312 (2003).
- [22] M. A. Levin and X.-G. Wen, String-net condensation: A physical mechanism for topological phases, Physical Review B **71**, 045110 (2005).
- [23] A. Kitaev, Fault-tolerant quantum computation by anyons, Annals of Physics **303**, 2 (2003).
- [24] S. Aaronson and D. Gottesman, Improved simulation of stabilizer circuits, Physical Review A **70**, 052328 (2004).
- [25] D. Dong and I. R. Petersen, Quantum control theory and applications: a survey, IET Control Theory & Applications **4**, 2651 (2010).
- [26] H. R. Lewis Jr and W. Riesenfeld, An exact quantum theory of the time-dependent harmonic oscillator and of a charged particle in a time-dependent electromagnetic field, Journal of Mathematical Physics **10**, 1458 (1969).
- [27] R. Kaushal and S. Mishra, Dynamical algebraic approach and invariants for time-dependent hamiltonian systems in two dimensions, Journal of Mathematical Physics **34**, 5843 (1993).
- [28] H. Korsch, Dynamical invariants and time-dependent harmonic systems, Physics Letters A **74**, 294 (1979).
- [29] D. Guéry-Odelin, A. Ruschhaupt, A. Kiely, E. Torrontegui, S. Martínez-Garaot, and J. G. Muga, Shortcuts to adiabaticity: Concepts, methods, and applications, Reviews of Modern Physics **91**, 045001 (2019).
- [30] X. Chen, A. Ruschhaupt, S. Schmidt, A. del Campo, D. Guéry-Odelin, and J. G. Muga, Fast optimal frictionless atom cooling in harmonic traps: Shortcut to adiabaticity, Physical Review Letters **104**, 063002 (2010).
- [31] E. Torrontegui, S. Martínez-Garaot, and J. G. Muga, Hamiltonian engineering via invariants and dynamical algebra, Physical Review A **89**, 043408 (2014).
- [32] S. Simsek and F. Mintert, Quantum control with a multi-dimensional Gaussian quantum invariant, Quantum **5**, 409 (2021).
- [33] A. P. Peirce, M. A. Dahleh, and H. Rabitz, Optimal control of quantum-mechanical systems: Existence, numerical approximation, and applications, Physical Review A **37**, 4950 (1988).
- [34] F. Iachello, *Lie algebras and applications*, Vol. 708 (Springer, 2006).
- [35] C. P. Koch, U. Boscain, T. Calarco, G. Dirr, S. Filipp, S. J. Glaser, R. Kosloff, S. Montangero, T. Schulte-Herbrüggen, D. Sugny, and F. K. Wilhelm, Quantum optimal control in quantum technologies. Strategic report on current status, visions and goals for research in Europe, EPJ Quantum Technology **9**, 1 (2022).
- [36] V. F. Krotov, Global methods in optimal control theory, in *Advances in nonlinear dynamics and control: a report from Russia* (Springer, 1996) pp. 74–121.
- [37] M. Plesch and Č. Brukner, Quantum-state preparation with universal gate decompositions, Physical Review A **83**, 032302 (2011).
- [38] T. Albash and D. A. Lidar, Adiabatic quantum computation, Reviews of Modern Physics **90**, 015002 (2018).
- [39] E. Farhi, J. Goldstone, and S. Gutmann, A quantum approximate optimization algorithm, arXiv preprint arXiv:1411.4028 (2014).
- [40] P. Pfeuty, The one-dimensional Ising model with a transverse field, Annals of Physics **57**, 79 (1970).
- [41] G. B. Mbeng, A. Russomanno, and G. E. Santoro, The quantum ising chain for beginners, arXiv preprint arXiv:2009.09208 **114** (2020).
- [42] C. L. Degen, F. Reinhard, and P. Cappellaro, Quantum sensing, Reviews of Modern Physics **89**, 035002 (2017).
- [43] X.-R. Jin, X. Ji, Y.-Q. Zhang, S. Zhang, S.-K. Hong, K.-H. Yeon, and C.-I. Um, Three-party quantum secure direct communication based on GHZ states, Physics Let-

- ters A **354**, 67 (2006).
- [44] M. Hillery, V. Bužek, and A. Berthiaume, Quantum secret sharing, *Physical Review A* **59**, 1829 (1999).
- [45] F. Fröwis and W. Dür, Stable macroscopic quantum superpositions, *Physical Review Letters* **106**, 110402 (2011).
- [46] A. Omran, H. Levine, A. Keesling, G. Semeghini, T. T. Wang, S. Ebadi, H. Bernien, A. S. Zibrov, H. Pichler, S. Choi, *et al.*, Generation and manipulation of Schrödinger cat states in Rydberg atom arrays, *Science* **365**, 570 (2019).
- [47] C. Song, K. Xu, H. Li, Y.-R. Zhang, X. Zhang, W. Liu, Q. Guo, Z. Wang, W. Ren, J. Hao, *et al.*, Generation of multicomponent atomic Schrödinger cat states of up to 20 qubits, *Science* **365**, 574 (2019).
- [48] M. A. Nielsen, Cluster-state quantum computation, *Reports on Mathematical Physics* **57**, 147 (2006).
- [49] J. Hauschild and F. Pollmann, Efficient numerical simulations with tensor networks: Tensor Network Python (TeNPy), *SciPost Phys. Lect. Notes* , 5 (2018), code available from <https://github.com/tenpy/tenpy>, arXiv:1805.00055.
- [50] M. P. Zaletel, R. S. K. Mong, C. Karrasch, J. E. Moore, and F. Pollmann, Time-evolving a matrix product state with long-ranged interactions, *Physical Review B* **91**, 165112 (2015).
- [51] J. Preskill, Quantum computing in the NISQ era and beyond, *Quantum* **2**, 79 (2018).
- [52] S. Deffner and S. Campbell, Quantum speed limits: from Heisenberg’s uncertainty principle to optimal quantum control, *Journal of Physics A: Mathematical and Theoretical* **50**, 453001 (2017).
- [53] L. Gyongyosi and S. Imre, A survey on quantum computing technology, *Computer Science Review* **31**, 51 (2019).
- [54] Data for Orozco-Ruiz *et al.* “A way around the exponential scaling in optimal quantum control” (2024), DOI: 10.5281/zenodo.8298203.
- [55] A. Stern and N. H. Lindner, Topological quantum computation—from basic concepts to first experiments, *Science* **339**, 1179 (2013).
- [56] A. Paetznick, C. Knapp, N. Delfosse, B. Bauer, J. Haah, M. B. Hastings, and M. P. da Silva, Performance of planar floquet codes with majorana-based qubits, *PRX Quantum* **4**, 010310 (2023).
- [57] C. Gidney, M. Newman, A. Fowler, and M. Broughton, A fault-tolerant honeycomb memory, *Quantum* **5**, 605 (2021).
- [58] B. Srivastava, A. F. Kockum, and M. Granath, The XYZ<sup>2</sup> hexagonal stabilizer code, *Quantum* **6**, 698 (2022).
- [59] G. Wendin, Quantum information processing with superconducting circuits: a review, *Reports on Progress in Physics* **80**, 106001 (2017).
- [60] S. Ebadi, T. T. Wang, H. Levine, A. Keesling, G. Semeghini, A. Omran, D. Bluvstein, R. Samajdar, H. Pichler, W. W. Ho, *et al.*, Quantum phases of matter on a 256-atom programmable quantum simulator, *Nature* **595**, 227 (2021).
- [61] J. Carrasco, A. Elben, C. Kokail, B. Kraus, and P. Zoller, Theoretical and Experimental Perspectives of Quantum Verification, *PRX Quantum* **2**, 010102 (2021).
- [62] D. G. Cory, M. Price, W. Maas, E. Knill, R. Laflamme, W. H. Zurek, T. F. Havel, and S. S. Somaroo, Experimental quantum error correction, *Physical Review Letters* **81**, 2152 (1998).
- [63] J. Chiaverini, D. Leibfried, T. Schaetz, M. D. Barrett, R. Blakestad, J. Britton, W. M. Itano, J. D. Jost, E. Knill, C. Langer, *et al.*, Realization of quantum error correction, *Nature* **432**, 602 (2004).
- [64] F. Sauvage and F. Mintert, Optimal quantum control with poor statistics, *PRX Quantum* **1**, 020322 (2020).